environmental microbiology sfam

An antibacterial T6SS in *Pantoea agglomerans* pv. *betae* delivers a lysozyme-like effector to antagonize competitors

Andrea Carobbi[1] | Simone Di Nepi[1] | Chaya M. Fridman[2] | Yasmin Dar[2] |

Rotem Ben-Yaakov[2] | Isaac Barash[1] | Dor Salomon[2] [ID] | Guido Sessa[1] [ID]

[1]School of Plant Sciences and Food Security, The George S. Wise Faculty of Life Sciences, Tel-Aviv University, Tel-Aviv

[2]Department of Clinical Microbiology and Immunology, Sackler Faculty of Medicine, Tel Aviv University, Tel Aviv

Correspondence
Dor Salomon, Department of Clinical Microbiology and Immunology, Sackler Faculty of Medicine, Tel Aviv University, 6997801 Tel Aviv, Israel.
Email: dorsalomon@mail.tau.ac.il

Guido Sessa, School of Plant Sciences and Food Security, The George S. Wise Faculty of Life Sciences, Tel-Aviv University, 69978 Tel-Aviv, Israel.
Email: guidos@tauex.tau.ac.il

Abstract

The type VI secretion system (T6SS) is deployed by numerous Gram-negative bacteria to deliver toxic effectors into neighbouring cells. The genome of *Pantoea agglomerans* pv. *betae* (*Pab*) phytopathogenic bacteria contains a gene cluster (T6SS1) predicted to encode a complete T6SS. Using secretion and competition assays, we found that T6SS1 in *Pab* is a functional antibacterial system that allows this pathogen to outcompete rival plant-associated bacteria found in its natural environment. Computational analysis of the T6SS1 gene cluster revealed that antibacterial effector and immunity proteins are encoded within three genomic islands that also harbour arrays of orphan immunity genes or toxin and immunity cassettes. Functional analyses indicated that VgrG, a specialized antibacterial effector, contains a C-terminal catalytically active glucosaminidase domain that is used to degrade prey peptidoglycan. Moreover, we confirmed that a bicistronic unit at the end of the T6SS1 cluster encodes a novel antibacterial T6SS effector and immunity pair. Together, these results demonstrate that *Pab* T6SS1 is an antibacterial system delivering a lysozyme-like effector to eliminate competitors, and indicate that this bacterium contains additional novel T6SS effectors.

INTRODUCTION

The type VI secretion system (T6SS) is a contact-dependent toxin delivery apparatus that is widespread among Gram-negative bacteria (Bingle et al., 2008; Coulthurst, 2019; Filloux et al., 2008; Wang et al., 2019). It is composed of 14 conserved proteins (TssA-M and a PAAR repeat-containing protein) that are often encoded by large gene clusters (Boyer et al., 2009; Shneider et al., 2013). The T6SS delivers toxins, called effectors, directly into bacterial and eukaryotic cells (Jurėnas & Journet, 2021). Structurally, the T6SS is similar to a contractile phage tail (Nguyen et al., 2018; Wang et al., 2019). Contraction of an outer

sheath tube propels an inner tube, which is decorated with effectors, out of the bacterial cell and into immediately adjacent cells (Basler & Mekalanos, 2012). This secreted tail tube consists of stacked hexameric rings of the Hcp protein (TssD), which are capped with a spike made of a trimer of valine-glycine repeat proteins (VgrG/TssI) bound to a Proline-Alanine–Alanine-aRginine (PAAR) repeat-containing protein that sharpens it (Nguyen et al., 2018; Shneider et al., 2013).

T6SS effectors can be either toxin domains that are fused to the tail tube components Hcp, VgrG and PAAR, and referred to as specialized effectors, or proteins that are non-covalently bound to the tail tube components and defined as cargo effectors (Jurėnas & Journet, 2021). Depending on the nature of its effector arsenal, the T6SS mediates interbacterial competition and/or contributes to

Andrea Carobbi and Simone Di Nepi contributed equally to this work.

virulence against eukaryotes (Hachani et al., 2016; Jana & Salomon, 2019; Jurėnas & Journet, 2021; Monjarás & Valvano, 2020). T6SS antibacterial effectors may act in the periplasm or in the cytoplasm of the prey cell; they carry diverse toxin domains that target vital bacterial cell components, such as nucleic acids, the cell wall and the membrane (e.g. Jana & Salomon, 2019; LaCourse et al., 2018; Ma et al., 2014; Miyata et al., 2013; Russell et al., 2011; Russell et al., 2012). T6SS effectors that target eukaryotic cell processes and contribute to bacterial virulence have also been reported (e.g. Pukatzki et al., 2006; Jiang et al., 2014; Hachani et al., 2016; Chen et al., 2017; Ray et al., 2017; Monjarás & Valvano, 2020). Interestingly, certain T6SSs have been shown to deliver both antibacterial and virulence effectors, thus implicating them in both bacterial competition and host manipulation (Jiang et al., 2014; MacIntyre et al., 2010; Pukatzki et al., 2006; Ray et al., 2017). Numerous effector families have been identified to date (e.g. Ahmad et al., 2019; Dar et al., 2018; de Moraes et al., 2021; Durand et al., 2014; Hernandez et al., 2020; Jana et al., 2019; Nolan et al., 2021; Russell et al., 2013; Salomon et al., 2014; Tang et al., 2018; Ting et al., 2018; Wood et al., 2019) and it is likely that many additional families remain unknown. To avoid T6SS-mediated self-intoxication, bacteria encode immunity proteins, which provide protection against the effectors' toxicity; the corresponding genes are adjacent to their cognate effector genes in bicistronic units (Hood et al., 2010; Whitney et al., 2013). Immunity proteins localize to the cellular compartment of action of the cognate effectors and they generally appear to neutralize the effectors rather than protect the target. In fact, in many instances they have been shown to bind to the catalytic domain of effectors and occlude their binding site or lock them in an inactive conformation (Jurėnas & Journet, 2021; Ruhe et al., 2020).

T6SSs are also widely distributed in genomes of bacterial plant pathogens such as *Pseudomonas*, *Xanthomonas*, *Ralstonia*, *Agrobacterium* and *Erwinia* (Bayer-Santos et al., 2019; Bernal et al., 2018; Boyer et al., 2009; Wu et al., 2018; Wu et al., 2021); yet until recently they have received much less attention than their counterparts in animal pathogens (Bernal et al., 2018). In many of these organisms, the T6SS does not appear to be primarily used against the plant host, but rather against other members of the microbial community inhabiting the same environmental niche. Several T6SSs of plant pathogenic bacteria were shown to play a role in interbacterial competition, such as in *Pseudomonas syringae* (Haapalainen et al., 2012), *Acidovorax citrulli* (Levy et al., 2018), *Agrobacterium tumefaciens* (Ma et al., 2014) and *Pantoea ananatis* (Shyntum et al., 2015). However, in most cases the function and biochemical properties of putative secreted effectors were not investigated. Remarkably, non-pathogenic bacteria have been proposed as biocontrol agents to inhibit plant pathogens and prevent

diseases (Bernal et al., 2018; Cassan et al., 2021). In support of this possibility, *Pseudomonas putida* KT2440, whose genome includes three T6SS gene clusters, was shown to outcompete plant pathogens in vitro and *in planta* in a T6SS-dependent manner (Bernal et al., 2018).

Pantoea agglomerans (*Pa*) is an epiphytic and endophytic bacterium widespread in diverse natural and agricultural habitats (Kobayashi & Palumbo, 2000; Lindow & Brandl, 2003). Strains of *Pa* have evolved into tumorigenic pathogens displaying host specificity on various plants by acquiring a pathogenicity plasmid, which contains genes encoding structural components and effectors of the type III secretion system, enzymes of auxin and cytokinins biosynthesis, and multiple insertion sequences (Barash & Manulis-Sasson, 2009; Guo et al., 2002). *Pa* strains inflict important losses in beet (*Beta vulgaris*) crops used for human consumption and sugar industry (Burr et al., 1991), and prevent root development of gypsophila (*Gypsophila paniculata*) cuttings employed for flower production (Cooksey, 1986). Two *Pa* pathogenic pathovars were identified: *Pa* pv. *gypsophilae* (*Pag*) and *Pa* pv. *betae* (*Pab*) (Burr et al., 1991). *Pag* causes development of galls on gypsophila and triggers a hypersensitive response on beet. *Pab* causes galls on beet as well as on gypsophila, albeit galls on gypsophila caused by *Pab* are morphologically distinguishable from galls caused by *Pag* (Burr et al., 1991).

The presence of a T6SS in the genome of *Pa* phytopathogenic strains, its functionality, and possible contribution to interbacterial competition remain unexplored. In addition, the repertoire and biochemical activity of *Pa* T6SS effectors are largely unknown. In this study, we provide evidence that the *Pab* genome contains a T6SS gene cluster, T6SS1, which encodes a complete set of T6SS core components and accessory proteins, as well as effectors and immunity genes found within evolving genomic islands. By functional analyses, we demonstrate that T6SS1 is competent in effectors secretion and plays a role in antibacterial competition that may contribute to *Pab* establishment in its environmental niche. We also show that *Pab* VgrG is a specialized T6SS effector, which induces peptidoglycan degradation leading to cell lysis, and is antagonized by its cognate immunity, Vgi. Lastly, we identify a novel antibacterial effector and immunity pair.

EXPERIMENTAL PROCEDURES

Bacterial strains and media

The bacterial strains used are *Pantoea agglomerans* pv. *betae* strain 4188 (*Pab*), *Agrobacterium tumefaciens* GV3101 (Han et al., 2013), *Xanthomonas campestris* pv. *campestris* strain B100 (Hötte et al., 1990),

Escherichia coli strains DH5α *λpir* (a gift from Eric V. Stabb) and MG1655 (Edwards & Palsson, 2000). *Pantoea agglomerans*, *A. tumefaciens* and *X. campestris* were grown in Lysogeny Broth (LB) medium at 28°C; *E. coli* were grown in LB or 2×YT medium at 37°C. Media were supplemented with ampicillin (50 μg/ml), spectinomycin (50 μg/ml), rifampicin (100 μg/ml), streptomycin (50 μg/ml), tetracycline (13 μg/ml) or chloramphenicol (35 μg/ml), as required.

T6SS cluster analysis

Pab T6SS gene clusters were identified by homology searches using T6SS components that were previously reported in other *Pantoea* strains (De Maayer et al., 2011). Analyses of domains encoded by genes located in the *hcp*, *vgrG* and *paar* islands were performed using the NCBI Conserved Domain Database (Lu et al., 2020) and hidden Markov modelling (HHpred; Zimmermann et al., 2018). Homologues in other bacterial strains were identified using BLAST (Altschul et al., 1990), and their genomic neighbourhoods were analysed manually.

VgrG^Tox amino acid conservation

One round of PSI-BLAST (Altschul et al., 1997) was used to identify 500 proteins homologous to the VgrG C-terminal toxin domain (amino acids 675–829; VgrG^Tox). The retrieved sequences were aligned in MEGA X (Kumar et al., 2018) using MUSCLE (Edgar, 2004). Aligned columns not found in VgrG were discarded. The amino acid conservation of the homologues was illustrated using the WebLogo 3 server (http://weblogo.threeplusone.com; Crooks et al., 2004). The putative active site of the VgrG toxic domain was determined as E752 based on amino acid sequence comparison with the *Salmonella typhimurium* FlgJ peptidoglycan hydrolase (Zaloba et al., 2016).

Pse2 amino acid conservation

Three rounds of PSI-BLAST (Altschul et al., 1997) were used to identify 500 proteins homologous to Pse2. The retrieved sequences were aligned in MEGA X (Kumar et al., 2018) using MUSCLE (Edgar, 2004). Aligned columns not found in Pse2 were discarded. The amino acid conservation of the homologues was illustrated using the WebLogo 3 server (http://weblogo.threeplusone.com; Crooks et al., 2004). Secondary structures were predicted with Jpred4 (Drozdetskiy et al., 2015) using the Pse2 sequence; transmembrane helices were predicted with the Phobius server (Käll et al., 2004).

Pab growth assays

Pab and its mutant derivative strains were grown overnight in LB at 28°C, diluted to $OD_{600} = 0.01$, and then 200 μl of each sample was transferred into 96-well plates in triplicates. OD_{600} values were measured every 10 min for 7 h while plates were grown at 28°C with agitation (205 cpm) in a microplate reader (BioTek SYNERGY H1).

Plasmid construction

For expression in *E. coli*, genes encoding *tssA* (A7P61_RS17205), *vgrG* (A7P61_RS17105), *vgrG^Core*, *vgrG^Tox*, *vgi* (A7P61_RS17100), *pse2* (A7P61_RS17025), *psi2* (A7P61_RS17020) were amplified from *Pab* genomic DNA. By using the Gibson assembly method (Gibson et al., 2009), amplicons were inserted in the multiple cloning site (MCS) of one of the following arabinose-inducible plasmids: pBAD/*Myc*–6His (hereafter referred to as pBAD), or pPER5/*Myc*–6His (hereafter referred to as pPER5), a pBAD derivative carrying the PelB signal peptide sequence at the 5′ of the MCS (Dar et al., 2021), or pBAD33.1 (Chung & Raetz, 2010). All inserted genes were positioned in frame with a 3′-encoded *Myc*–6His tag. The obtained plasmids were transformed into *E. coli* MG1655 using the electroporation method.

For expression in *Pab*, the *hcp* (A7P61_RS17185), *tssA* (A7P61_RS17205), *pse2* (A7P61_RS17025) and *psi2* (A7P61_RS17020) genes were PCR-amplified from *Pab* genomic DNA and inserted in the MCS of the pBBR1-MCS-3 (Kovach et al., 1995) or pBAD plasmids. The obtained plasmids were transformed into *E. coli* DH5α *λpir* using the heat shock method (Froger & Hall, 2007), and then introduced into *Pab* bacteria by triparental mating using the conjugation helper strain *E. coli* DH5α carrying the helper plasmid pBR2073 (Figurski & Helinski, 1979). When an arabinose-inducible vector was used, transformants were grown on LB agar plates or liquid cultures supplemented by 0.4% (wt./vol.) glucose to repress expression from the *Pbad* promoter.

Site-directed mutagenesis

To generate the *vgrG^{E752A}* mutant, site-directed mutagenesis was performed using as template the *vgrG* gene cloned in the pPER5 plasmid, as described by Edelheit et al. (2009). *vgrG* was amplified in two separate reactions of asymmetric PCR using either a forward or reverse primer carrying a Glu to Ala substitution at position 752. Reaction products were combined, denatured at 95°C, reannealed and digested by *Dpn*I restriction enzyme to remove

methylated parental DNA. The product was then directly transformed in *E. coli* MG1655.

Protein expression in *E. coli*

Escherichia coli MG1655 cells carrying arabinose-inducible expression plasmids pBAD or pPER5 were grown overnight at 28°C in 3 ml of LB supplemented with appropriate antibiotics and 0.4% (wt./vol.) glucose. Cultures were normalized to $OD_{600} = 0.1$ and grown for 2 h at 28°C. Cells were then washed with LB to remove residual glucose, and 0.1% (wt./vol.) L-arabinose was added to the media to induce protein expression. Cultures were grown for 2 or 4 h at 28°C as necessary, and 0.25 OD_{600} units of cells were pelleted and resuspended in 40 μl (2×) Tris-Glycine sodium dodecyl sulfate (SDS) sample buffer (Novex, Life Sciences) supplemented with 0.05% (wt./vol.) β-mercaptoethanol. Samples were boiled and cell lysates were fractionated by SDS-PAGE, transferred onto PDVF membranes, and immunoblotted with α-Myc (Santa Cruz Biotechnology, 9E10, mouse mAb) antibodies, used at 1:1000 dilution.

Bacterial toxicity assays

Escherichia coli MG1655 cells transformed with arabinose-inducible expression plasmids pBAD or pPER5 harbouring a kanamycin-resistance cassette (Fridman et al., 2020) or co-transformed with pPER5 and pBAD33.1 harbouring a chloramphenicol-resistance cassette were grown overnight at 28°C in 2×YT supplemented with appropriate antibiotics and 0.4% (wt./vol.) glucose to repress expression from the *Pbad* promoter. Cultures were washed with 2×YT to remove residual glucose and normalized to $OD_{600} = 0.01$ in 2×YT supplemented with the appropriate antibiotics. Next, 200 μl of each sample was transferred into 96-well plates in quadruplicates and grown at 28° in a BioTeck SYNERGY H1 microplate reader with agitation (205 cpm). After 2 h, L-arabinose was added to each well at a final concentration of 0.05% (wt./vol.) to induce protein expression, and plates were re-inserted into the microplate reader for 5 h additional incubation. OD_{600} values were measured every 10 min.

Generation of *Pab* deletion strains

To generate deletions of the *Pab tssA*, *vgrG* and *pse2* genes, of the *pse2* gene together with the cognate immunity gene *psi2*, and of the *vgrG* region encoding the C-terminal toxin domain either alone or together with its cognate immunity gene *vgi*, sequences located 1 kb upstream and 1 kb downstream of the region to be deleted, were PCR-amplified and inserted into the MCS of pDM4, a CmROriR6K suicide plasmid (Milton et al., 1996). The obtained plasmids were transformed into *E. coli* DH5α *λpir* by electroporation (Lessard, 2013). Transformants were used to transfer the construct into *Pab* by triparental mating using the helper strain *E. coli* DH5α carrying pBR2073. An initial selection of colonies was carried out on LB agar plates supplemented with chloramphenicol. Growing colonies were then transferred to LB agar plates supplemented with sucrose [15% (wt./vol.)] for counter-selection and loss of the SacB-containing pDM4, as described (Salomon et al., 2013). Deletions were confirmed by PCR and sequencing.

Bacterial competition assays

Attacker and prey bacterial strains were grown overnight in LB or 2×YT supplemented with the appropriate antibiotics. Bacterial cultures were normalized to $OD_{600} = 0.5$ (*Pab* and derivative strains) or $OD_{600} = 0.5$ (*E. coli*, *A. tumefaciens* and *X. campestris*) and mixed at a 4:1 (attacker:prey) volume ratio. Mixtures were spotted on LB agar plates with or without the addition of 0.1% (wt./vol.) L-arabinose to induce expression from plasmids, and incubated at 28°C. Colony-forming units (CFUs) of prey spotted at $t = 0$ h were determined by plating 10-fold serial dilutions on selective agar plates. To determine prey CFU at later timepoints, bacterial spots were scraped from agar plates into 1 ml LB. Next, 10-fold serial dilutions were plated on selective agar plates and CFUs were calculated. Antibiotic resistance used to select prey cells was as follows: for *X. campestris*, natural streptomycin resistance; for *A. tumefaciens*, spectinomycin resistance carried on the pER8b plasmid; and for *Pab*, chloramphenicol resistance carried on the pBAD33.1 plasmid.

Protein secretion assays

Protein secretion assays were performed as previously described (Fridman et al., 2020), with minor modifications. Briefly, *Pab* strains were grown overnight in LB supplemented with antibiotics, when required. The cultures were normalized to $OD_{600} = 0.1$ in 5 ml of LB supplemented with appropriate antibiotics and 0.005% (wt./vol.) L-arabinose, and grown for 5 h at 28°C. For extraction of cellular proteins (cells fraction), 0.25 OD_{600} units were collected, and cell pellets were resuspended in 40 μl of reducing protein sample buffer (2×; 100 mM Tris/HCl pH = 7.0, 20% glycerol, 25% SDS, bromophenol blue, 0.05% β-mercaptoethanol). The remaining culture volume (media fraction) was filtered (0.22 μm) and precipitated by addition of deoxycholate (150 μg/ml) followed by 8% trichloroacetic acid (Bensadoun & Weinstein, 1976). Precipitated proteins were washed twice with cold acetone and resuspended in 20 μl of

10 mM Tris/HCl pH = 8.0. An equal volume of 2× protein sample buffer and 1 μl NaOH 5 N were added to each sample. Samples were boiled and then resolved on SDS-PAGE, transferred onto PDVF membranes and immunoblotted with α-Myc or α-FLAG (Santa Cruz Biotechnology, F1804, mouse mAb) antibodies used at a 1:1000 dilution. RNA polymerase β (RNAp) was detected with Direct-Blot™ HRP α-*E. coli* RNA Sigma 70 (mouse mAb #663205; BioLegend; referred to as α-RNAp) and was used as a non-secreted protein to confirm equal loading of samples of total cell extracts and exclude contamination of supernatant fractions with cytoplasmic proteins (Dar et al., 2021).

Microscopy

To determine the effect of protein expression in *E. coli*, overnight *E. coli* MG1655 cells carrying pPER5-based plasmids were diluted 100-fold into 3 ml of fresh LB supplemented with kanamycin 30 mg/ml and 0.4% (wt./vol.) glucose. After 2 h incubation at 30°C, cells were washed twice with 0.15 M NaCl and normalized to OD_{600} = 1.5. For peptidoglycan visualization, cells were stained with Wheat Germ Agglutinin Alexa Fluor 488 Conjugate (Biotium; Catalogue no. 29022–1) at a final concentration of 0.1 mg/ml, and incubated for 10 min at room temperature (RT). Then, 1 μl of each culture was spotted onto LB agarose pads [1% (wt./vol.) agarose supplemented with 30 mg/ml kanamycin and 0.2% (wt./vol.) L-arabinose) to which 1 μl of the membrane-impermeable DNA dye, propidium iodide (PI; 1 mg/ml; Sigma-Aldrich), was pre-applied. After the spots dried (1–2 min at RT), the agarose pads were mounted, facing down, onto 35 mm glass-bottom CELLview™ cell culture dishes (Greiner). Cells were then imaged every 5 min for 3 h under a fluorescence microscope, as detailed below. The stage chamber (Okolab) temperature was set to 30°C. The following setup was used for imaging: a Nikon Eclipse Ti2E inverted motorized microscope with a CFI PLAN apochromat DM 100× oil lambda PH-3 (NA, 1.45) objective lens, a Lumencor SOLA SE II 395 light source, an ET-dsRED (#49005, CHROMA, to visualize PI signal) and ET-EGFP (#49002, CHROMA, to visualize GFP signal) filter sets, and a DS-QI2 Mono cooled digital microscope camera (16 MP). Obtained images were further processed and analysed using Fiji ImageJ suite (Schindelin et al., 2012).

RESULTS

The *Pab* genome contains a T6SS gene cluster with diverse effector and immunity genes

To characterize the T6SS in *Pantoea agglomerans* pv. *betae* (*Pab*), we first identified gene clusters in the *Pab* genome that encode known T6SS components. Analysis of the *Pab* assembled genome (NCBI RefSeq: NZ_LXSW01000076.1) revealed that it contains two conserved T6SS gene clusters previously named T6SS1 and T6SS2 (De Maayer et al., 2011) (Figure 1). The T6SS1 cluster encodes a complete T6SS, whereas T6SS2 encodes only a few system components.

hcp island

T6SS1 includes the previously described *hcp* island between the *hcp* and *tagH* genes (Table 1; Figure 1; Supporting Information Figure S1) (De Maayer et al., 2011). The two genes downstream of *hcp* (locus numbers A7P61_RS17180 and A7P61_RS 17175) are predicted to encode an antibacterial effector and its cognate immunity, which we named Pse1 (*Pab* type six effector 1) and Psi1 (*Pab* type six immunity 1), respectively. Pse1 is similar to pore-forming colicin toxins (97.2% probability of similarity between Pse1 amino acids 102–325 and amino acids 8–197 of the Colicin B C-terminal domain according to HHpred; Gabler et al., 2020) and its homologues often contain N-terminal domains found in polymorphic T6SS specialized effectors, such as PAAR (e.g. WP_047722894.1) or VgrG (e.g. WP_013660774.1). The gene downstream of *psi1* (A7P61_RS17170) encodes a member of the Tai4 family of immunity proteins (Russell et al., 2012). Interestingly, homologues of this gene are present immediately downstream of genes encoding Tae4 antibacterial effectors within the T6SS1 *hcp* island of other *Pantoea* strains (e.g. WP_182686054.1 in *Pantoea agglomerans* strain RSO7). The gene downstream of *tai4* (A7P61_RS17165) is a small open reading frame similar to Adhesin Complex Protein from *Neisseria meningitidis*, a predicted lysozyme inhibitor (Humbert et al., 2017) (92.95% probability of similarity between A7P61_RS17165 amino acids 2–119 and amino acids 1–120 of WP_002225721.1 according to HHpred). Homologues of this gene are found in *Pantoea hcp* islands immediately downstream of a gene encoding a putative antibacterial effector containing endolysin, a peptidoglycan-targeting toxin domain (e.g. WP_115064794.1 in *Pantoea agglomerans* strain LMAE-2); therefore, this gene possibly encodes an immunity protein. The two genes upstream of *tagH* (A7P61_RS17160 and A7P61_RS17155) both encode proteins containing the lysozyme inhibitor LprI domain (according to NCBI Conserved Domain Database; Marchler-Bauer et al., 2007), homologues of which are found in *Pantoea hcp* islands immediately downstream of an antibacterial effector containing a lysozyme-like toxin domain (e.g. WP_090962028.1 in *Pantoea* sp. OV426), and could therefore encode immunity
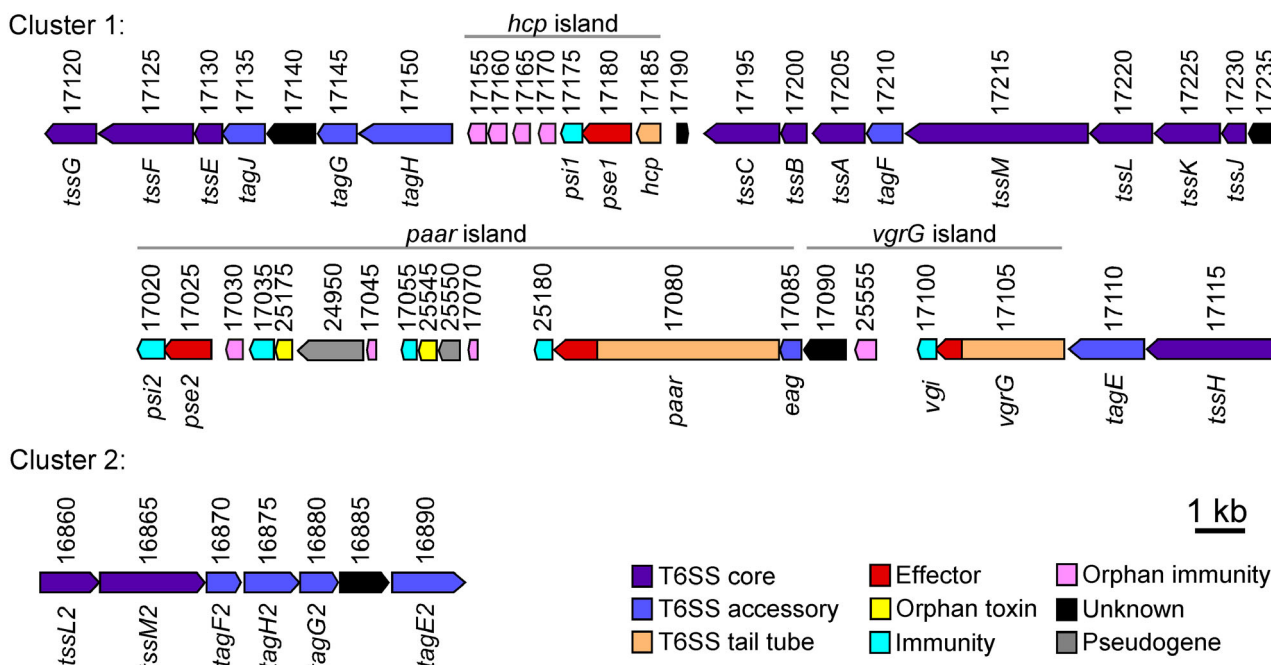
FIGURE 1   The *Pab* T6SS gene clusters. Schematic representation of T6SS gene clusters present in the *Pab* 4188 genome. Genes are represented by arrows indicating the direction of transcription. Locus tags (A7P61_RSxxxxx) are denoted above. Gene names are shown below. Black lines denote islands encoding putative effector and immunity proteins

proteins. These observations indicate that the *Pab hcp* island contains a pore-forming toxin and its cognate immunity, as well as four orphan immunity proteins that were possibly maintained through rounds of effector gene acquisition or acquired to provide immunity against peptidoglycan-targeting effectors deployed by competing *Pantoea* strains.

vgrG island

The *Pab vgrG* island (Table 1; Figure 1; Supplementary Figure S1) includes a gene encoding a specialized VgrG effector (A7P61_RS17105) that harbours a C-terminal extension domain predicted to be a member of the glucosaminidase superfamily of peptidoglycan-targeting toxins. We predict that the gene downstream of the *vgrG* gene (A7P61_RS17100) encodes its cognate immunity protein, which we named Vgi (V̲grG g̲lucosaminidase i̲mmunity). The gene downstream of *vgrG* and its putative cognate immunity gene (A7P61_RS25555) is a homologue of genes found immediately downstream of specialized VgrG effectors in other *Pantoea* strains and contain a C-terminal glycosyl hydrolase 108 toxin domain (e.g. WP_111142272.1 in *Pantoea* sp. ARC607); therefore, it is predicted to encode an immunity protein. We were unable to predict a role for the protein encoded by the A7P61_RS17090 gene.

paar island

The gene upstream of the gene encoding the PAAR domain-containing protein (hereafter, referred to as PAAR), A7P61_RS17085, encodes a protein with a DcrB domain (Table 1; Figure 1; Supporting Information Figure S1). This domain was previously referred to as DUF1795 or Eag and it serves as an adaptor for T6SS specialized effectors (Alcoforado Diniz & Coulthurst, 2015; Cianfanelli et al., 2016). In addition to a PAAR domain, the PAAR-encoding gene (A7P61_RS17080) also encodes RhsA repeats (Koskiniemi et al., 2013) and a C-terminal extension that harbours a putative antibacterial toxin domain similar to previously described Tne2 NADase toxins (Tang et al., 2018) (99.7% probability between amino acids 1365–1487 of PAAR and amino acids 14–132 of Tne2 from *Pseudomonas fluorescens* Pf-5 according to HHpred). Homologues of this C-terminal domain are found in diverse *Proteobacteria*, where they are fused to PAAR and RhsA domains, and in *Firmicutes*, where they are fused to TANFOR domains, which were recently shown to carry polymorphic toxins (e.g. WP_066428025) (Jana et al., 2020; Quentin et al., 2018). Therefore, the PAAR protein appears to be a specialized effector. In agreement with the prediction that the PAAR C-terminal domain is a putative antibacterial toxin, a small gene (A7P61_RS25180), which potentially encodes a cognate immunity protein, is found immediately downstream to it.

TABLE 1 Putative effectors and immunity genes located in the *Pab* T6SS1 gene cluster

Island	Accession number	Locus	Domains	Predicted activity
hcp	WP_064704484.1	A7P61_RS17180	Pore-forming colicin-like (H)	Antibacterial effector (Pse1)
	WP_064704483.1	A7P61_RS17175	TMH (P)	Immunity protein (Psi1)
	WP_064704482.1	A7P61_RS17170	Tai4 amidase immunity (N); SP (P)	Orphan immunity protein
	WP_064704481.1	A7P61_RS17165	Lysozyme inhibitor-like (N); SP (P)	Orphan immunity protein
	WP_064704845.1	A7P61_RS17160	Lysozyme inhibitor LprI (N); SP (P)	Orphan immunity protein
	WP_231115776.1	A7P61_RS17155	Lysozyme inhibitor LprI (N); SP (P)	Orphan immunity protein
vgrG	WP_064704473.1	A7P61_RS17105	VgrG (N); Glucosaminidase superfamily (N)	Specialized antibacterial effector
	WP_060680008.1	A7P61_RS17100	SP (P)	Immunity protein (Vgi)
	WP_064704843.1	A7P61_RS25555	SP (P)	Orphan immunity protein
	WP_064704472.1	A7P61_RS17090	SP (P)	Unknown
paar	WP_064704471.1	A7P61_RS17085	DcrB superfamily (N)	Adaptor
	WP_064704470.1	A7P61_RS17080	PAAR (N); RhsA (N); Tne2-like NADase toxin (H)	Specialized antibacterial effector
	WP_064704469.1	A7P61_RS25180	Unknown	Immunity protein
	WP_064704468.1	A7P61_RS17070	Unknown	Orphan immunity protein
	Pseudogene	A7P61_RS25550	N/A	N/A
	WP_064704466.1	A7P61_RS25545	Unknown	Orphan toxin domain
	WP_197980968.1	A7P61_RS17055	Unknown	Immunity protein
	WP_010246002.1	A7P61_RS17045	Enterocin A Immunity (H)	Orphan immunity protein
	Pseudogene	A7P61_RS24950	N/A	N/A
	WP_196766544.1	A7P61_RS25175	Nuclease (H)	Orphan toxin domain
	WP_064704463.1	A7P61_RS17035	RhsI1-like (H)	Immunity protein
	WP_064704462.1	A7P61_RS17030	Unknown	Orphan immunity protein
	WP_064704461.1	A7P61_RS17025	TMH (P)	Antibacterial effector (Pse2)
	WP_064704460.1	A7P61_RS17020	TMH (P)	Immunity protein (Psi2)

Abbreviations: H, predicted using HHpred (Zimmermann et al., 2018); N, predicted using NCBI Conserved Domain Database (Marchler-Bauer et al., 2007); N/A, Not applicable; P, predicted using Phobius (Käll et al., 2004); SP, signal peptide; TMH, transmembrane helix.

Close inspection of the 3′ end of the T6SS1 gene cluster led us to conclude that the previous assessment of the *Pantoea* T6SS1 cluster borders (De Maayer et al., 2011) was incomplete; we determined that the cluster does not end immediately after the PAAR-encoding gene, but rather it extends downstream to the A7P61_RS17020 gene. We termed the region spanning from the adaptor-encoding gene upstream of the PAAR protein (A7P61_RS17085) to the A7P61_17020 gene as 'paar island' (Table 1; Figure 1; Supporting Information Figure S1). Analysis of the genes present in this island revealed several putative orphan toxin-immunity modules; this phenomenon was previously described downstream of other Rhs-containing polymorphic toxins (Koskiniemi et al., 2013). The A7P61_RS17070 gene encodes a homologue of proteins encoded immediately downstream of PAAR proteins at the same position in clusters of other *Pantoea* strains (e.g. WP_132498480.1 in *Pantoea agglomerans* strain MM2021_7), and therefore it is possibly an orphan immunity protein. The A7P61_RS25550 gene, which is annotated as a pseudogene, appears to encode a region of an RhsA-containing protein missing its N-terminal region and a C-terminal toxin domain. The downstream genes, A7P61_RS25545 and

A7P61_RS17055, encode homologues of a C-terminal predicted toxin domain fused to a specialized PAAR protein and its neighbouring immunity protein at the same position in clusters of other *Pantoea* strains (e.g. WP_085068094.1 and WP_085068093.1 in *Pantoea alhagi* strain LTYR-226 11Z. Therefore, these two genes possibly represent another orphan toxin-immunity module that can be fused via DNA rearrangement to the PAAR encoded at the beginning of the *paar* island. The A7P61_RS17045 gene encodes another putative orphan immunity protein, as it is identical to a putative immunity protein encoded immediately downstream of a Rhs-containing PAAR protein that is at the same position of the *Pab* PAAR in the *paar* island, but in a different *Pantoea* strain (e.g. WP_010246002.1 in *Pantoea agglomerans* strain L15). It is similar to the immunity protein of the bacteriocin Enterocin A (93.53% probability between amino acids 5–73 of A7P61_RS17045 and amino acids 1–71 of a protein belonging to pfam group PF08951). A7P61_RS24950, which is also annotated as an Rhs-encoding pseudogene, appears to encode a protein missing both its N-terminal region and toxin-containing C-terminal region. Interestingly, the downstream A7P61_RS25175 gene encodes a protein displaying homology to
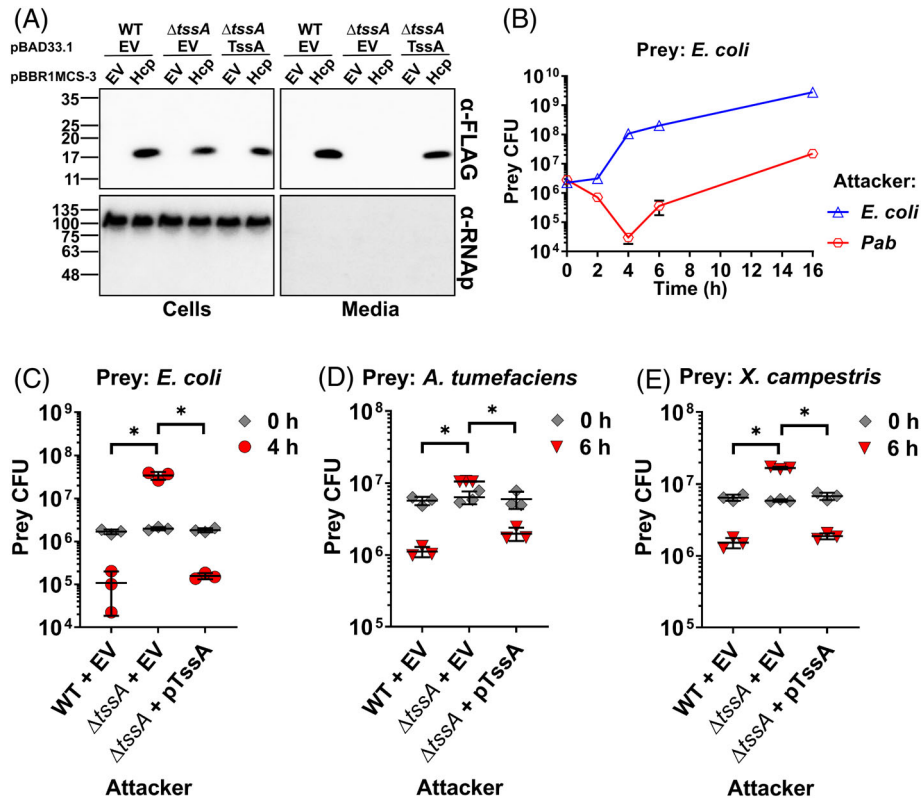
FIGURE 2 The *Pab* T6SS is a functional antibacterial system. (A) Expression (cells) and secretion (media) of FLAG-tagged Hcp from *Pab* wild-type (WT) and Δ*tssA* mutant (Δ*tssA*) strains carrying the indicated plasmids were detected by immunoblotting using α-FLAG antibodies. RNA polymerase β was detected with α-RNAp antibodies and used to confirm equal loading in cells samples and to verify the absence of contamination of supernatant fractions with cytoplasmic proteins. TssA was expressed from the arabinose-inducible plasmid, pBAD33.1. The experiment was repeated three times with similar results. Results from a representative experiment are shown. (B) Viability counts of *E. coli* MG1655 prey at the indicated timepoints when co-incubated with either *E. coli* or *Pab* attackers. (C–E) Viability counts of the prey strains *E. coli* MG1655 (C), *Agrobacterium tumefaciens* GV3101 (D) and *Xanthomonas campestris* pv. *campestris* 8100 (E) before (0 h) and after (4 h for *E. coli*; 6 h for *A. tumefaciens* and *X. campestris*) co-incubation with *Pab* WT and Δ*tssA* attackers carrying a plasmid either empty (EV) or expressing TssA (pTssA). Data are shown as the mean ± SD of three biological replicates. Asterisks denote statistical significance between samples at $t = 4$ h or $t = 6$ h by an unpaired, two-tailed Student's t-test ($p < 0.01$)

the C-terminus of Rhs-containing PAAR proteins of other *Pantoea* strains (e.g. WP_062757477.1 in *Pantoea agglomerans* NBRC 102470), and to the putative C-terminal nuclease domain of RhsA_2 from *Serratia marcescens* (99.89% probability between amino acids 1–103 of A7P61_RS17045 and amino acids 52–154 of the toxin domain in the PDB structure 6XTD, corresponding to accession number SAY43811.1; according to HHpred), and is therefore possibly a toxin. As expected, the downstream A7P61_RS17035 gene encodes a homologue of the protein encoded downstream of the above-mentioned toxin and it is predicted to be its cognate immunity protein (100% probability between amino acids 1–163 of A7P61_RS17035 and amino acids 2–163 of the immunity protein in the PDB structure 6XTD; according to HHpred). The A7P61_RS17030 gene may also encode an orphan immunity protein since it is homologous to a protein encoded immediately downstream of an Rhs-containing gene found downstream of an Rhs-containing PAAR in other bacteria (e.g. WP_013036149.1 in *Erwinia amylovora* CFBP1430). The last two genes in this island

(A7P61_RS17025 and A7P61_RS17020, which we named *pse2* and *psi2*, respectively, as explained below), encode proteins that do not contain any described domain; however, their organization in a bicistronic operon and their position within the *paar* island suggest that they encode either an effector and immunity pair, or an orphan toxin-immunity module. The latter possibility is less likely since we did not identify homologues of the putative effector, which is encoded by the A7P61_RS17025 gene, fused to known N-terminal domains of polymorphic toxins.

Taken together, these observations indicate that the *Pab* T6SS1 cluster contains three evolving islands that accumulate arrays of orphan immunity and toxin-immunity modules. This possibly confers *Pab* the ability to resist aggression by *Pantoea* relatives that carry diverse T6SS effector repertoires, as well as allows *Pab* to evolve new effectors of its own by replacing the C-terminal toxin domain fused to the PAAR protein with toxin-immunity module present in the array downstream to it.

Pab T6SS1 is a functional antibacterial system

To determine whether the T6SS1 cluster encodes a functional T6SS, we set out to monitor secretion of the hallmark-secreted tail tube component Hcp (Mougous et al., 2006). To this end, we first constructed a T6SS mutant by deleting the gene encoding the conserved structural component TssA (Planamente et al., 2016; Shyntum et al., 2015). As shown in Figure 2(A) (upper panels), FLAG-tagged Hcp expressed from a plasmid was secreted from wild-type *Pab* grown under standard laboratory conditions (i.e. LB at 28°C), but not from the ΔtssA mutant. Complementation of TssA from a plasmid restored Hcp secretion. This result demonstrates that the *Pab* T6SS1 is functional under laboratory conditions.

Our analysis of the T6SS1 gene cluster revealed several putative antibacterial effector and immunity pairs. Therefore, we hypothesized that this system plays a role in interbacterial competition. To test this hypothesis, we determined the outcome of co-incubation of *Pab* with *E. coli* MG1655 as potential sensitive prey. As shown in Figure 2(B), the viability of the *E. coli* prey decreased over time upon co-incubation with wild-type *Pab*, but not when *E. coli* was co-incubated with the equivalent numbers of *E. coli* attackers (*E. coli* prey contained a kanamycin resistance selective marker distinguishing it from its parental *E. coli* attackers); the decrease in *E. coli* viability reached a maximum after 4 h of co-incubation with *Pab*, followed by an increase in the *E. coli* prey CFU, which could be attributed to phase separation that protected pockets of *E. coli* populations (McNally et al., 2017). To determine whether the loss of *E. coli* viability was mediated by the *Pab* T6SS1, we co-incubated *E. coli* prey with either wild-type *Pab* or the ΔtssA mutant, and monitored its viability after 4 h. As expected, loss of *E. coli* viability was detected when it was co-incubated with wild-type *Pab* but not with the ΔtssA mutant [Figure 2(C)], indicating that T6SS1 is responsible for the antibacterial effect. Deletion of the *tssA* gene did not affect *Pab* bacterial growth (Supporting Information Figure S2). Notably, complementation of TssA from a plasmid restored the antibacterial activity of the ΔtssA mutant [Figure 2(C)].

Since *E. coli* is not commonly found in the *Pab* natural environmental niche, the rhizosphere (i.e. soil and plant roots), we tested whether the *Pab* T6SS1 can also mediate the killing of plant-associated bacteria. To this end, we monitored the viability of *Agrobacterium tumefaciens* and *Xanthomonas campestris* pv. *campestris* upon co-incubation with *Pab*. As shown in Figure 2(D) and (E), *Pab* efficiently killed both prey bacteria. This antibacterial activity was mediated by T6SS1, since it was abolished when the ΔtssA mutant was used [Figure 2(D) and (E)]. Taken together, these

results demonstrate that the *Pab* T6SS1 is an antibacterial system that is used to eliminate bacterial competitors.

VgrG is a specialized antibacterial effector targeting the peptidoglycan

We set out to investigate antibacterial effector and immunity pairs that are encoded within the T6SS1 gene cluster. We first focused on VgrG and its cognate immunity Vgi. As mentioned above, the *Pab* VgrG is a specialized effector that contains a C-terminal extension domain predicted to be a member of the glucosaminidase superfamily [Figure 3(A); amino acids
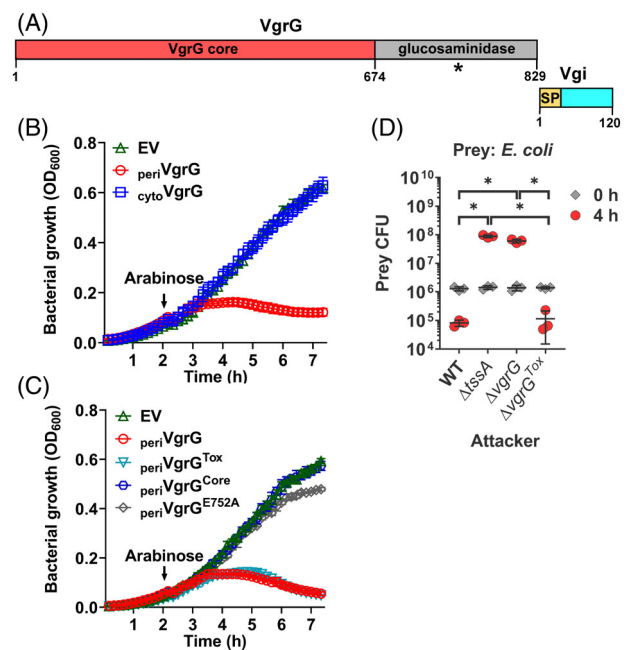

FIGURE 3 The C-terminus of VgrG contains an antibacterial toxin. (A) Schematic representation of *Pab* VgrG and its cognate immunity protein Vgi. Domains and amino acid positions of note are denoted. An asterisk indicates the position of the conserved E752 amino acid residue. SP, signal peptide. (B–C) Growth of *E. coli* MG1655 containing arabinose-inducible plasmids for the expression of cytoplasmic (cyto) or periplasmic (peri) VgrG (B), and periplasmic VgrG derivatives (C), including the VgrG glucosaminidase domain (amino acids 675–829; peri VgrG^{Tox}), the VgrG core (amino acids 1–674; peri VgrG^{Core}) and VgrG carrying a substitution of the conserved E752 to Ala (peri VgrG^{E752A}). Protein expression was induced after 2 h of growth by the addition of 0.05% ʟ-arabinose (denoted by an arrow). Data are shown as the mean ± SD ($n = 4$ technical replicates) from a representative experiment. Experiments were repeated three times with similar results. (D) Viability counts of *E. coli* MG1655 prey before (0 h) and after (4 h) co-incubation with the attacker strains *Pab* wild-type (WT), *Pab* ΔtssA mutant (ΔtssA), *Pab* ΔvgrG mutant (ΔvgrG), or *Pab* with a deletion in the region encoding the VgrG glucosaminidase domain (ΔvgrG^{Tox}). Data are shown as the mean ± SD of three biological replicates. Asterisks denote statistical significance between samples at $t = 4$ h by an unpaired, two-tailed Student's t-test ($p < 0.01$)

675–829]. The presence of this domain suggests that the VgrG effector hydrolyses the peptidoglycan in the bacterial periplasm. In agreement with this prediction, the putative cognate immunity protein Vgi, which is encoded by the gene downstream of *vgrG*, has an N-terminal signal peptide for periplasmic localization (according to the SignalP 5.0 prediction server; Almagro Armenteros et al., 2019) [Figure 3(A)]. To investigate whether VgrG is an antibacterial toxin, we expressed it in *E. coli* as a surrogate host from an arabinose-inducible plasmid, either in its natural form (cytoVgrG) or fused to an N-terminal PelB signal peptide (periVgrG), for periplasmic localization. As shown in Figure 3(B), only the periplasmic version was toxic in agreement with its predicted activity as a peptidoglycan hydrolyzing toxin. Induction of periVgrG expression resulted in a decline in the OD_{600} readings, which is compatible with cell lysis.

Next, we determined whether the C-terminal glucosaminidase domain is responsible for the toxicity observed when VgrG was delivered to the *E. coli* periplasm. Indeed, expression of the glucosaminidase domain (amino acids 675–829; periVgrG^{Tox}), but not of the N-terminal structural part of VgrG (amino acids 1–674; periVgrG^{Core}), was sufficient to cause the observed decline in the OD_{600} of the *E. coli* culture [Figure 3(C)]. Analysis of protein sequences homologous to the VgrG C-terminal toxin domain (Supporting Information Figure S3) revealed a conserved glutamic acid (E752) that corresponds to an annotated active site residue in another member of the glucosaminidase family, the peptidoglycan-hydrolyzing flagellar component, FlgJ (UniProtKB – P75942; Boutet et al., 2007). In agreement with this C-terminal domain being the toxin, and with its predicted activity as a member of the glucosaminidase superfamily, substitution of the conserved E752 to alanine (periVgrG^{E752A}) abolished the toxicity of VgrG in *E. coli* [Figure 3(C)]. The expression of all VgrG versions in *E. coli* was confirmed by immunoblotting, aside from the toxic C-terminal domain whose expression was not detected. To further confirm that the C-terminal glucosaminidase domain of VgrG is a toxin domain that is not required for the structural role of VgrG as an essential part of the T6SS tail tube, we constructed *Pab* mutant strains in which we deleted either the entire *vgrG* gene (Δ*vgrG*) or only the region encoding the C-terminal glucosaminidase domain (Δ*vgrG^{Tox}*). We then used these mutants as attackers in a competition assay against *E. coli* prey. Deletion of the entire *vgrG* gene abolished T6SS-mediated antibacterial activity, similar to deletion of the conserved component *tssA* [Figure 3(D)]. However, deletion of the C-terminal toxin domain alone did not affect the antibacterial activity against *E. coli* prey, indicating that the T6SS remained functional and delivered other antibacterial effectors even in the absence of the specialized toxin domain fused to VgrG.

The toxicity of VgrG in the *E. coli* periplasm and the reduction in the optical density of the *E. coli* culture upon its expression [Figure 3(B)] supported the predicted activity of the C-terminal toxin domain as a peptidoglycan hydrolase. To assess this predicted activity, we monitored the effect of periplasmic expression of VgrG on cell morphology and the peptidoglycan layer of *E. coli* under the microscope. Expression of VgrG induced cell rounding and lysis, together with apparent disappearance of the peptidoglycan layer (Figure 4 top panel; Supporting Information Movie S1). The catalytically inactive VgrG mutant (VgrG^{E752A}) had no effect on cell morphology or the peptidoglycan over time (Figure 4 middle panel; Supporting Information Movie S2), and it was comparable to an empty expression plasmid (Figure 4 bottom panel; Supporting Information Movie S3). Taken together, these results suggest that VgrG is a specialized antibacterial effector with a C-terminal glucosaminidase toxin domain that hydrolyses peptidoglycan leading to cell lysis. Interestingly, we found that homologues of VgrG encoded by other *Pantoea* strains contain one of at least five C-terminal toxin domains. Aside from the glucosaminidase domain present in the *Pab* VgrG, other homologues contain LytD, glycosyl hydrolase 108, lysozyme-like, or metallopeptidase C-terminal
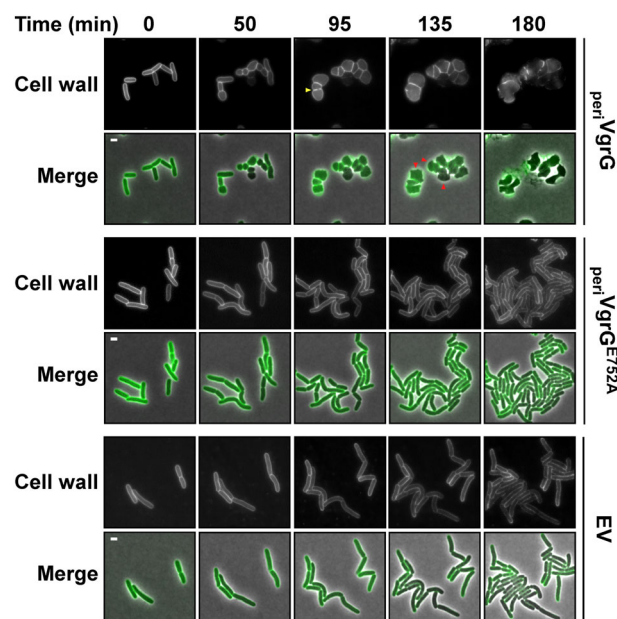

FIGURE 4 VgrG induces cell wall degradation leading to cell lysis in *E. coli*. Time-lapse microscopy of *E. coli* cells expressing periplasm-targeted VgrG (periVgrG), a catalytic mutant (periVgrG^{E752A}), or containing an empty arabinose-inducible expression vector (EV). Cells stained with Wheat Germ Agglutinin Alexa Fluor 488 Conjugate (cell wall stain; green in merged panels) were spotted on LB agarose pads supplemented with kanamycin and 0.2% arabinose. Merging of the phase contrast and GFP channels (for Alexa Fluor 488 visualization) and only the GFP channel are shown. A yellow arrowhead denotes cell wall stain that disappears in the following time frame. Red arrowheads denote cells that are lysed in the following time frame. Scale bar = 2 μm

domains (Supporting Information Figure S5). Remarkably, these five domains are all predicted to target the peptidoglycan.

Vgi antagonizes the toxicity mediated by VgrG

We predicted that the gene downstream of *vgrG*, encoding Vgi, is its cognate immunity gene. As expected from an immunity against a toxin that functions in the periplasm, Vgi has a predicted signal peptide. To investigate the ability of Vgi to antagonize VgrG-mediated toxicity, we first expressed both proteins, either together or alone, in *E. coli*. As shown in Figure 5(A), Vgi rescued *E. coli* from VgrG-mediated toxicity when periplasm localized VgrG and Vgi were coexpressed. In addition, we tested whether VgrG and Vgi function as a T6SS antibacterial effector and immunity pair. To this end, we generated a *Pab* mutant in which we deleted the *vgrG* region encoding the C-terminal toxin domain together with the *vgi* gene ($\Delta vgrG^{Tox}$-*vgi*). This deletion did not affect *Pab* growth (Supporting Information Figure S2). We then used this mutant strain as prey in competition against *Pab* attackers. The deletion rendered the mutant susceptible to intoxication by a wild-type *Pab* attacker, but not by the T6SS1-deficient attackers $\Delta tssA$ and $\Delta vgrG$ [Figure 5(B)], indicating that a gene providing immunity against T6SS-mediated attack was deleted in this prey. A $\Delta vgrG^{Tox}$ attacker, which still retains ability to intoxicate *E. coli* prey [Figure 3(D)], was unable to intoxicate

the mutant *Pab* prey, demonstrating that the intoxicating effector was the C-terminal toxin domain in the specialized VgrG. Importantly, expression of Vgi from an arabinose-inducible plasmid restored the ability of the $\Delta vgrG^{Tox}$-*vgi* prey to resist intoxication by a wild-type *Pab* attacker [Figure 5(B)]. Therefore, the results show that VgrG and Vgi are a bona fide T6SS antibacterial effector and immunity pair.

Pse2 is a T6SS-delivered antibacterial effector that is antagonized by Psi2

In the analysis of the *Pab* T6SS1 gene cluster, we hypothesized that the two genes at the 3′ end of the cluster, encoding Pse2 and Psi2, are a T6SS effector and immunity pair. To test this hypothesis, we first determined whether Pse2 is secreted in a T6SS-dependent manner. Immunoblotting of Pse2 expressed from a plasmid revealed its presence in the supernatant of wild-type *Pab*, but not in the supernatant of $\Delta tssA$ *Pab* [Figure 6(A), upper panels]. This result confirms that Pse2 is a secreted substrate of T6SS1.

Next, we tested whether Pse2 and Psi2 function as a T6SS antibacterial effector and immunity pair during interbacterial competition. To this end, we generated a *Pab* mutant in which we deleted both *pse2* and *psi2* genes ($\Delta pse2$-*psi2*). This deletion did not affect *Pab* growth [Supporting Information Figure S6(A)]. We then used this mutant strain as prey in competition against *Pab* attackers. The deletion rendered the mutant susceptible to intoxication by a wild-type *Pab* attacker, but not by the T6SS1 deficient attacker $\Delta tssA$ [Figure 6(B)], indicating that a gene providing immunity against T6SS-mediated attack was deleted in this prey. A $\Delta pse2$ attacker, which still retains ability to intoxicate *E. coli* prey [Supporting Information Figure S6(B)], was unable to intoxicate the mutant *Pab* prey, demonstrating that Pse2 was the intoxicating effector. Remarkably, expression of Psi2 from an arabinose-inducible plasmid restored the ability of the $\Delta pse2$-*psi2* prey to resist intoxication by a wild-type *Pab* attacker [Figure 6(B)]. Therefore, the results show that Pse2 and Psi2 are a bona fide T6SS1 antibacterial effector and immunity pair.

Both Pse2 and Psi2 contain predicted transmembrane helices (according to Phobius web server predictions; Käll et al., 2004) [Supporting Information Figure S6(C)], suggesting that the putative effector Pse2 functions in the bacterial membrane or periplasm. To determine whether Pse2 mediates antibacterial toxicity in the periplasm, we expressed it from an arabinose-inducible plasmid in *E. coli*, either in its natural form ($_{cyto}$Pse2) or fused to an N-terminal PelB signal peptide ($_{peri}$Pse2), for periplasmic localization. As shown in Figure 6(C), only the periplasmic version was toxic. Furthermore, coexpression of
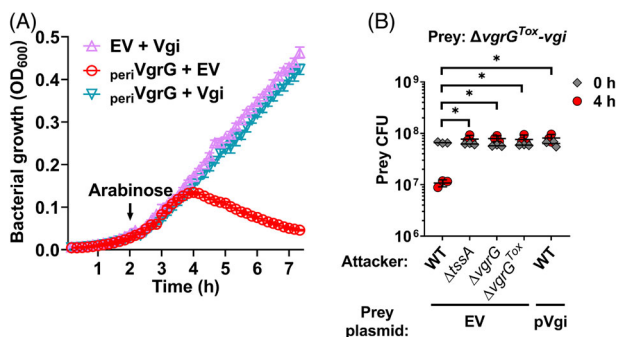

FIGURE 5 Vgi antagonizes VgrG-mediated toxicity. (A) Growth of *E. coli* MG1655 containing arabinose-inducible plasmids for coexpression of periplasmic VgrG ($_{peri}$VgrG) and Vgi. Empty vectors (EV) were used as control. Protein expression was induced after 2 h of growth by the addition of 0.05% L-arabinose (denoted by an arrow). Data are shown as the mean $\pm$ SD ($n = 4$ technical repeats). (B) Viability counts of *Pab* mutant lacking the VgrG glucosaminidase domain and the downstream *vgi* gene ($\Delta vgrG^{Tox}$-*vgi*), and carrying a plasmid either empty (EV) or for arabinose-inducible expression of Vgi (pVgi), before (0 h) and after (4 h) co-incubation with the indicated *Pab* attackers on LB agar containing 0.05% L-arabinose. Data are shown as the mean $\pm$ SD of three biological replicates. Asterisks denote statistical significance between samples at $t = 4$ h by an unpaired, two-tailed Student's *t*-test ($p < 0.01$)
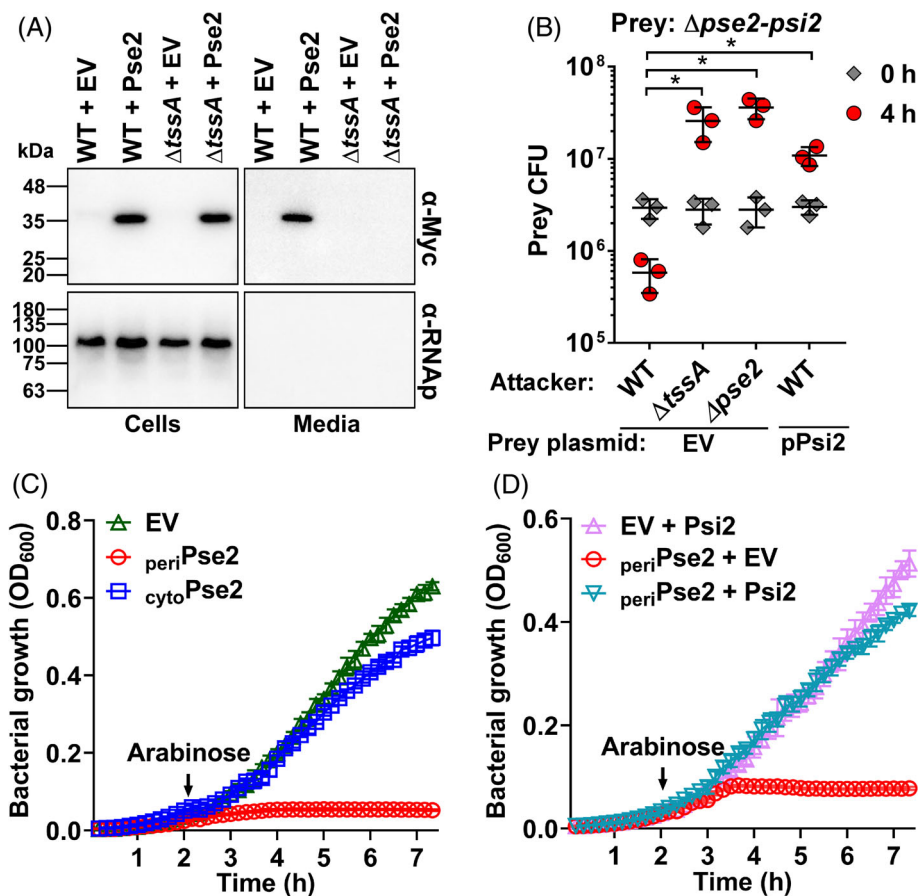
FIGURE 6 Pse2 and Psi2 are an antibacterial effector and immunity pair. (A) Expression (cells) and secretion (media) of Pse2 from *Pab* wild-type (WT) and Δ*tssA* mutant (Δ*tssA*) strains carrying a plasmid for arabinose-inducible expression of C-terminal Myc-tagged Pse2 or an empty vector (EV). Pse2-Myc was detected by immunoblotting using α-Myc antibodies. RNA polymerase β was detected with α-RNAp antibodies and used to confirm equal loading in cells samples and to verify the absence of contamination of supernatant fractions with cytoplasmic proteins. (B) Viability counts of *Pab* mutant lacking the *pse2* and *psi2* genes (Δ*pse2-psi2*), and carrying a plasmid either empty (EV) or for arabinose-inducible expression of Psi2 (pPsi2), before (0 h) and after (4 h) co-incubation with the indicated *Pab* attackers on LB agar containing 0.05% ʟ-arabinose. Asterisks denote statistical significance between samples at $t = 4$ h by an unpaired, two-tailed Student's *t*-test ($p < 0.01$). (C–D) Growth of *E. coli* MG1655 containing arabinose-inducible plasmids for the expression of C-terminal Myc-tagged cytoplasmic (cyto) or periplasmic (peri) Pse2 (C), or periplasmic Pse2 together with Psi2 (D). Empty vectors (EV) were used as control. Protein expression was induced after 2 h growth by the addition of 0.05% ʟ-arabinose (denoted by an arrow). Data are shown as the mean ± SD ($n = 4$ technical repeats). In each panel, experiments were repeated three times with similar results. Results from a representative experiment are shown

Psi2 rescued *E. coli* from Pse2-mediated toxicity [Figure 6(D)]. The expression of the cytoplasmic and periplasmic versions of Pse2 was confirmed by immunoblotting [Supporting Information Figure S6 (D)]. Consistent with its toxic activity, the accumulation of the periplasmic Pse2 was detected when coexpressed with its cognate immunity protein Psi2, but not when expressed alone [Supporting Information Figure S6(D)].

DISCUSSION

We identified a functional T6SS cluster (T6SS1) in the genome of *Pab* phytopathogenic bacteria mediating antibacterial activity and enabling *Pab* to outcompete several bacterial species that co-inhabit the rhizosphere niche. *Pab* also contains an auxiliary T6SS gene cluster, named T6SS2, encoding additional copies of T6SS core and accessory proteins. Clusters with a genetic composition similar to *Pab* T6SS1 and T6SS2 have been previously reported to be conserved in the genome of *Pantoea ananatis* and *Erwinia* species, while an additional cluster, named T6SS3, is present in a subset of *Pantoea* and *Erwinia* strains but absent in *Pab* (De Maayer et al., 2011; Shyntum et al., 2014). The role of T6SS components found in the partial T6SS2 cluster, and whether or not the corresponding genes are expressed, remain to be investigated. Since the gene content and organization of the T6SS2 cluster appear to be conserved in *Pab* and *P. ananatis* strains (Shyntum et al., 2014), it is likely that T6SS2 serves a functional purpose favouring its retention in the genus. It is possible that T6SS2 and

T6SS1 components function together to form a derivative T6SS apparatus.

We identified antibacterial effector and immunity gene pairs encoded in three evolving islands (*hcp*, *vgrG* and *paar*) within the T6SS1 gene cluster. A distinctive characteristic of the composition of the *hcp* island is the presence of an effector immunity gene pair downstream of the *hcp* gene followed by an array of putative orphan immunity genes. This gene organization possibly evolved as a result of consecutive integration events of effector and cognate immunity genes by a yet-to-be-defined mechanism of horizontal gene transfer between *Pantoea* and *Erwinia* strains. We hypothesize that integration of each new module replaced a previous effector gene, while the previous immunity gene was retained downstream of the newly integrated cassette. Therefore, the array of orphan immunity genes present in the *Pab hcp* island may originate from multiple events of effector and immunity integration and effector displacement, possibly maintaining immunity against attacks by other kin strains in which the replaced effectors are still functional. Similar genetic rearrangements were previously proposed as the evolutionary dynamics that generated arrays of multiple different orphan immunity genes in T6SS clusters of *V. cholerae* strains (Kirchberger et al., 2017). A similar phenomenon can be also envisaged for the origin and function of the orphan immunity gene present in the *vgrG* island downstream of the *vgrG* and cognate immunity genes.

An alternative mechanism of effector diversification can be found in the *paar* island. The conserved effector in this island is a PAAR domain-containing protein that harbours Rhs repeats and a toxin domain fused to the C-terminal end of the protein; the toxin domain differs between *Pantoea* strains. Similar to previously reported Rhs proteins (Ma et al., 2017), the downstream regions of the *Pantoea* Rhs effectors harbour various orphan toxin and immunity modules that have the potential to recombine into the main PAAR-Rhs-encoding gene, thus giving rise to different specialized effectors than can outcompete their parental kin. However, it cannot be excluded that orphan toxins encoded in the *paar* island are secreted as cargo effectors. Notably, some of the orphan toxin and immunity modules in *Pab paar* islands appear to have been deactivated by frame-shift or non-sense mutations (i.e. pseudogenes). Taken together, these observations indicate that the *Pab* T6SS1 cluster is rapidly evolving and likely to drive strain diversification. We propose that in a sense, the *hcp* and *vgrG* islands record the evolutionary effector history of the strain, whereas the *paar* island contains information of possible future effectors.

The *vgrG* gene of *Pab* bacteria encodes an evolved form of the VgrG tail component with a C-terminal putative glucosaminidase extension. This extension is missing in *P. ananatis* strains with a single *vgrG* copy, but present in an additional *vgrG* gene of *P. ananatis* strains with two *vgrG* copies (Shyntum et al., 2014). Based on computational analyses, we predicted that the VgrG C-terminal domain encodes a peptidoglycan-hydrolyzing toxin that targets a periplasmic component of prey cells. Indeed, a combination of genetic, toxicity and microscopy assays supported this hypothesis. Notably, the presence of peptidoglycan-hydrolyzing toxin domains in homologues of VgrG identified in other *Pantoea* strains suggests that the role of this effector in targeting the cell wall of a competing cell is an important aspect of this T6SS, and this activity is thus conserved.

We found a novel effector and immunity pair, Pse2/Psi2, which is encoded at the 3′ end of the *paar* island. Although the activity and specific target(s) of the antibacterial effector Pse2 remain unknown, the presence of transmembrane helices in its amino acid sequence suggests that it could target the bacterial membrane, possibly by forming pores. It is also probable that other effectors are encoded outside of the *Pab* T6SS1 cluster, and that these can further diversify its antibacterial arsenal.

In conclusion, we identified a functional antibacterial T6SS and several effector and immunity pairs in *Pab* phytopathogenic bacteria. Future studies will aim to assess the contribution of *Pab* antibacterial activity to competitive fitness in the rhizosphere, and to determine whether this activity contributes directly or indirectly to *Pab* virulence towards the host plant.

CONFLICT OF INTEREST
The authors have no conflicts of interest to declare.

DATA AVAILABILITY STATEMENT
The data that supports the findings of this study is available in the figures, table and supplemental material of this article.

ORCID
Dor Salomon https://orcid.org/0000-0002-2009-9453
Guido Sessa https://orcid.org/0000-0001-8737-7377

REFERENCES
Ahmad, S., Wang, B., Walker, M.D., Tran, H.R., Stogios, P.J., Savchenko, A. et al. (2019) An interbacterial toxin inhibits target cell growth by synthesizing (p)ppApp. *Nature*, 575, 674–678.

Alcoforado Diniz, J. & Coulthurst, S.J. (2015) Intraspecies competition in *Serratia marcescens* is mediated by type VI-secreted Rhs effectors and a conserved effector-associated accessory protein. *Journal of Bacteriology*, 197, 2350–2360.

Almagro Armenteros, J.J., Tsirigos, K.D., Sønderby, C.K., Petersen, T.N., Winther, O., Brunak, S. et al. (2019) SignalP 5.0 improves signal peptide predictions using deep neural networks. *Nature Biotechnology*, 37, 420–423.

Altschul, S.F., Gish, W., Miller, W., Myers, E.W. & Lipman, D.J. (1990) Basic local alignment search tool. *Journal of Molecular Biology*, 215, 403–410.

Altschul, S.F., Madden, T.L., Schäffer, A.A., Zhang, J., Zhang, Z., Miller, W. et al. (1997) Gapped BLAST and PSI-BLAST: a new generation of protein database search programs. *Nucleic Acids Research*, 25, 3389–3402.

Barash, I. & Manulis-Sasson, S. (2009) Recent evolution of bacterial pathogens: the gall-forming *Pantoea agglomerans* case. *Annual Review of Phytopathology*, 47, 133–152.

Basler, M. & Mekalanos, J.J. (2012) Type 6 secretion dynamics within and between bacterial cells. *Science*, 337, 815.

Bayer-Santos, E., Ceseti, L.M., Farah, C.S. & Alvarez-Martinez, C.E. (2019) Distribution, function and regulation of type 6 secretion systems of *Xanthomonadales*. *Frontiers in Microbiology*, 10, 1635.

Bensadoun, A. & Weinstein, D. (1976) Assay of proteins in the presence of interfering materials. *Analytical Biochemistry*, 70, 241–250.

Bernal, P., Llamas, M.A. & Filloux, A. (2018) Type VI secretion systems in plant-associated bacteria. *Environmental Microbiology*, 20, 1–15.

Bingle, L.E., Bailey, C.M. & Pallen, M.J. (2008) Type VI secretion: a beginner's guide. *Current Opinion in Microbiology*, 11, 3–8.

Boutet, E., Lieberherr, D., Tognolli, M., Schneider, M. & Bairoch, A. (2007) UniProtKB/Swiss-Prot. *Methods in Molecular Biology*, 406, 89–112.

Boyer, F., Fichant, G., Berthod, J., Vandenbrouck, Y. & Attree, I. (2009) Dissecting the bacterial type VI secretion system by a genome wide in silico analysis: what can be learned from available microbial genomic resources? *BMC Genomics*, 10, 104.

Burr, T.J., Katz, B.H., Abawi, G.S. & Crosier, D.C. (1991) Comparison of tumorigenic strains of *Erwinia herbicola* isolated from table beet with *E. h. gypsophilae*. *Plant Disease*, 75, 855–858.

Cassan, F.D., Coniglio, A., Amavizca, E., Maroniche, G., Cascales, E., Bashan, Y. et al. (2021) The *Azospirillum brasilense* type VI secretion system promotes cell aggregation, biocontrol protection against phytopathogens and attachment to the microalgae *Chlorella sorokiniana*. *Environmental Microbiology*, 23, 6257–6274.

Chen, H., Yang, D., Han, F., Tan, J., Zhang, L., Xiao, J. et al. (2017) The bacterial T6SS effector EvpP prevents NLRP3 inflammasome activation by inhibiting the Ca^{2+}-dependent MAPK-Jnk pathway. *Cell Host & Microbe*, 21, 47–58.

Chung, H.S. & Raetz, C.R. (2010) Interchangeable domains in the Kdo transferases of *Escherichia coli* and *Haemophilus influenzae*. *Biochemistry*, 49, 4126–4137.

Cianfanelli, F.R., Alcoforado Diniz, J., Guo, M., De Cesare, V., Trost, M. & Coulthurst, S.J. (2016) VgrG and PAAR proteins define distinct versions of a functional type VI secretion system. *PLoS Pathogen*, 12, e1005735.

Cooksey, D.A. (1986) Galls of *Gypsophila paniculata* caused by *Erwinia herbicola*. *Plant Disease*, 70, 464–468.

Coulthurst, S. (2019) The type VI secretion system: a versatile bacterial weapon. *Microbiology*, 165, 503–515.

Crooks, G.E., Hon, G., Chandonia, J.M. & Brenner, S.E. (2004) WebLogo: a sequence logo generator. *Genome Research*, 14, 1188–1190.

Dar, Y., Salomon, D. & Bosis, E. (2018) The antibacterial and anti-eukaryotic type VI secretion system MIX-effector repertoire in *Vibrionaceae*. *Marine Drugs*, 16, 433.

Dar, Y., Jana, B., Bosis, E. & Salomon, D. (2021) A binary effector module secreted by a type VI secretion system. *EMBO Reports*, 9, e53981.

De Maayer, P., Venter, S.N., Kamber, T., Duffy, B., Coutinho, T. & Smits, T.H.M. (2011) Comparative genomics of the type VI secretion systems of *Pantoea* and *Erwinia* species reveals the presence of putative effector islands that may be translocated by the VgrG and Hcp proteins. *BMC Genomics*, 12, 576.

Drozdetskiy, A., Cole, C., Procter, J. & Barton, G.J. (2015) JPred4: a protein secondary structure prediction server. *Nucleic Acids Research*, 43, W389–W394.

Durand, E., Cambillau, C., Cascales, E. & Journet, L. (2014) VgrG, Tae, Tle, and beyond: the versatile arsenal of type VI secretion effectors. *Trends in Microbiology*, 22, 498–507.

Edelheit, O., Hanukoglu, A. & Hanukoglu, I. (2009) Simple and efficient site-directed mutagenesis using two single-primer reactions in parallel to generate mutants for protein structure-function studies. *BMC Biotechnology*, 9, 61.

Edgar, R.C. (2004) MUSCLE: multiple sequence alignment with high accuracy and high throughput. *Nucleic Acids Research*, 32, 1792–1797.

Edwards, J.S. & Palsson, B.O. (2000) The *Escherichia coli* MG1655 in silico metabolic genotype: its definition, characteristics, and capabilities. *Proceedings of the National Academy of Sciences of the United States of America*, 97, 5528–5533.

Figurski, D.H. & Helinski, D.R. (1979) Replication of an origin-containing derivative of plasmid RK2 dependent on a plasmid function provided in trans. *Proceedings of the National Academy of Sciences of the United States of America*, 76, 1648–1652.

Filloux, A., Hachani, A. & Bleves, S. (2008) The bacterial type VI secretion machine: yet another player for protein transport across membranes. *Microbiology*, 154, 1570–1583.

Fridman, C.M., Keppel, K., Gerlic, M., Bosis, E. & Salomon, D. (2020) A comparative genomics methodology reveals a widespread family of membrane-disrupting T6SS effectors. *Nature Communications*, 11, 1085.

Froger, A. & Hall, J.E. (2007) Transformation of plasmid DNA into *E. coli* using the heat shock method. *Journal of Visualized Experiments*, 6, 253.

Gabler, F., Nam, S.-Z., Till, S., Mirdita, M., Steinegger, M., Söding, J. et al. (2020) Protein sequence analysis using the MPI bioinformatics toolkit. *Current Protocols in Immunology*, 72, e108.

Gibson, D., Young, L., Chuang, R.Y., Venter, J.C., Hutchison, C.A., III & Smith, H. (2009) Enzymatic assembly of DNA molecules up to several hundred kilobases. *Nature Methods*, 6, 343–345.

Guo, M., Manulis, S., Mor, H. & Barash, I. (2002) The presence of diverse IS elements and an *avrPphD* homologue that acts as a virulence factor on the pathogenicity plasmid of *Erwinia herbicola* pv. *gypsophilae*. *Molecular Plant-Microbe Interactions*, 15, 709–716.

Haapalainen, M., Mosorin, H., Dorati, F., Wu, R.F., Roine, E., Taira, S. et al. (2012) Hcp2, a secreted protein of the phytopathogen *Pseudomonas syringae* pv. *tomato* DC3000, is required for fitness for competition against bacteria and yeasts. *Journal of Bacteriology*, 194, 4810–4822.

Hachani, A., Wood, T.E. & Filloux, A. (2016) Type VI secretion and anti-host effectors. *Current Opinion in Microbiology*, 29, 81–93.

Han, Z.F., Hunter, D.M., Sibbald, S., Zhang, J.S. & Tian, L. (2013) Biological activity of the tzs gene of nopaline *Agrobacterium tumefaciens* GV3101 in plant regeneration and genetic transformation. *Molecular Plant-Microbe Interactions*, 26, 1359–1365.

Hernandez, R.E., Gallegos-Monterrosa, R. & Coulthurst, S.J. (2020) Type VI secretion system effector proteins: effective weapons for bacterial competitiveness. *Cellular Microbiology*, 22, e13241.

Hood, R.D., Singh, P., Hsu, F., Güvener, T., Carl, M.A., Trinidad, R.R. et al. (2010) A type VI secretion system of *Pseudomonas aeruginosa* targets a toxin to bacteria. *Cell Host & Microbe*, 7, 25–37.

Hötte, B., Rath-Arnold, I., Pühler, A. & Simon, R. (1990) Cloning and analysis of a 35.3-kilobase DNA region involved in exopolysaccharide production by *Xanthomonas campestris* pv. *campestris*. *Journal of Bacteriology*, 172, 2804–2807.

Humbert, M.V., Awanye, A.M., Lian, L.Y., Derrick, J.P. & Christodoulides, M. (2017) Structure of the *Neisseria* Adhesin Complex Protein (ACP) and its role as a novel lysozyme inhibitor. *PLoS Pathogens*, 13, e1006448.

Jana, B. & Salomon, D. (2019) Type VI secretion system: a modular toolkit for bacterial dominance. *Future Microbiology*, 14, 1451–1463.

Jana, B., Fridman, C.M., Bosis, E. & Salomon, D. (2019) A modular effector with a DNase domain and a marker for T6SS substrates. *Nature Communications*, 10, 3595.

Jana, B., Salomon, D. & Bosis, E. (2020) A novel class of polymorphic toxins in Bacteroidetes. *Life Science Alliance*, 3, e201900631.

Jiang, F., Waterfield, N.R., Yang, J., Yang, G. & Jin, Q. (2014) A *Pseudomonas aeruginosa* type VI secretion phospholipase D effector targets both prokaryotic and eukaryotic cells. *Cell Host & Microbe*, 15, 600–610.

Jurėnas, D. & Journet, L. (2021) Activity, delivery, and diversity of type VI secretion effectors. *Molecular Microbiology*, 115, 383–394.

Käll, L., Krogh, A. & Sonnhammer, E.L. (2004) A combined transmembrane topology and signal peptide prediction method. *Journal of Molecular Biology*, 338, 1027–1036.

Kirchberger, P.C., Unterweger, D., Provenzano, D., Pukatzki, S. & Boucher, Y. (2017) Sequential displacement of type VI secretion system effector genes leads to evolution of diverse immunity gene arrays in *Vibrio cholerae*. *Scientific Reports*, 7, 45133.

Kobayashi, D.Y. & Palumbo, J.D. (2000) Bacterial endophytes and their effects on plants and uses in agriculture. In: Bacon, C.W. & White, J.J.F. (Eds.) *Microbial endophytes*. Basel, Switzerland: Marcel Dekker Inc, pp. 199–233.

Koskiniemi, S., Lamoureux, J.G., Nikolakakis, K.C., t'Kint de Roodenbeke, C., Kaplan, M.D., Low, D.A. et al. (2013) Rhs proteins from diverse bacteria mediates bacterial competition. *Proceedings of the National Academy of Sciences of the United States of America*, 110, 7032–7037.

Kovach, M.E., Elzer, P.H., Hill, D.S., Robertson, G.T., Farris, M.A., Roop, R.M., II et al. (1995) Four new derivatives of the broad-host-range cloning vector pBBR1MCS, carrying different antibiotic-resistance cassettes. *Gene*, 166, 175–176.

Kumar, S., Stecher, G., Li, M., Knyaz, C. & Tamura, K. (2018) MEGA X: molecular evolutionary genetics analysis across computing platforms. *Molecular Biology and Evolution*, 35, 1547–1549.

LaCourse, K.D., Peterson, S.B., Kulasekara, H.D., Radey, M.C., Kim, J. & Mougous, J.D. (2018) Conditional toxicity and synergy drive diversity among antibacterial effectors. *Nature Microbiology*, 3, 440–446.

Lessard, J.C. (2013) Transformation of *E. coli* via electroporation. *Methods in Enzymology*, 529, 321–327.

Levy, A., Salas Gonzalez, I., Mittelviefhaus, M., Clingenpeel, S., Herrera Paredes, S., Miao, J. et al. (2018) Genomic features of bacterial adaptation to plants. *Nature Genetics*, 50, 138–150.

Lindow, S.E. & Brandl, M.T. (2003) Microbiology of the phyllosphere. *Applied and Environmental Microbiology*, 69, 1875–1883.

Lu, S., Wang, J., Chitsaz, F., Derbyshire, M.K., Geer, R.C., Gonzales, N.R. et al. (2020) CDD/SPARCLE: the conserved domain database in 2020. *Nucleic Acids Research*, 48, D265–D268.

Ma, L.S., Hachani, A., Lin, J.S., Filloux, A. & Lai, E.M. (2014) *Agrobacterium tumefaciens* deploys a superfamily of type VI secretion DNase effectors as weapons for interbacterial competition in planta. *Cell Host & Microbe*, 16, 94–104.

Ma, J., Sun, M., Dong, W., Pan, Z., Lu, C. & Yao, H. (2017) PAAR-Rhs proteins harbor various C-terminal toxins to diversify the antibacterial pathways of type VI secretion systems. *Environmental Microbiology*, 19, 345–360.

MacIntyre, D.L., Miyata, S.T., Kitaoka, M. & Pukatzki, S. (2010) The *Vibrio cholerae* type VI secretion system displays antimicrobial properties. *Proceedings of the National Academy of Sciences of the United States of America*, 107, 19520–19524.

Marchler-Bauer, A., Anderson, J.B., Derbyshire, M.K., DeWeese-Scott, C., Gonzales, N.R., Gwadz, M. et al. (2007) CDD: a conserved domain database for interactive domain family analysis. *Nucleic Acids Research*, 35, D237–D240.

McNally, L., Bernardy, E., Thomas, J., Kalziqi, A., Pentz, J., Brown, S.P. et al. (2017) Killing by type VI secretion drives genetic phase separation and correlates with increased cooperation. *Nature Communications*, 8, 14371.

Milton, D.L., O'Toole, R., Horstedt, P. & Wolf-Watz, H. (1996) Flagellin A is essential for the virulence of *Vibrio anguillarum*. *Journal of Bacteriology*, 178, 1310–1309.

Miyata, S.T., Unterweger, D., Rudko, S.P. & Pukatzki, S. (2013) Dual expression profile of type VI secretion system immunity genes protects pandemic *Vibrio cholerae*. *PLoS Pathogens*, 9, e1003752.

Monjarás, F.J. & Valvano, M.A. (2020) An overview of anti-eukaryotic T6SS effectors. *Frontiers in Cellular and Infection Microbiology*, 10, 584751.

de Moraes, M.H., Hsu, F., Huang, D., Bosch, D.E., Zeng, J., Radey, M.C. et al. (2021) An interbacterial DNA deaminase toxin directly mutagenizes surviving target populations. *eLife*, 10, e62967.

Mougous, J.D., Cuff, M.E., Raunser, S., Shen, A., Zhou, M., Gifford, C.A. et al. (2006) A virulence locus of *Pseudomonas aeruginosa* encodes a protein secretion apparatus. *Science*, 312, 1526–1530.

Nguyen, V.S., Douzi, B., Durand, E., Roussel, A., Cascales, E. & Cambillau, C. (2018) Towards a complete structural deciphering of type VI secretion system. *Current Opinion in Structural Biology*, 49, 77–84.

Nolan, L.M., Cain, A.K., Clamens, T., Furniss, R.C.D., Manoli, E., Sainz-Polo, M.A. et al. (2021) Identification of Tse8 as a type VI secretion system toxin from *Pseudomonas aeruginosa* that targets the bacterial transamidosome to inhibit protein synthesis in prey cells. *Nature Microbiology*, 6, 1199–1210.

Planamente, S., Salih, O., Manoli, E., Albesa-Jové, D., Freemont, P.S. & Filloux, A. (2016) TssA forms a gp6-like ring attached to the type VI secretion sheath. *The EMBO Journal*, 35, 1613–1627.

Pukatzki, S., Ma, A.T., Sturtevant, D., Krastins, B., Sarracino, D., Nelson, W.C. et al. (2006) Identification of a conserved bacterial protein secretion system in *Vibrio cholerae* using the *Dictyostelium* host model system. *Proceedings of the National Academy of Sciences of the United States of America*, 103, 1528–1533.

Quentin, D., Ahmad, S., Shanthamoorthy, P., Mougous, J.D., Whitney, J.C. & Raunser, S. (2018) Mechanism of loading and translocation of type VI secretion system effector Tse6. *Nature Microbiology*, 3, 1142–1152.

Ray, A., Schwartz, N., de Souza Santos, M., Zhang, J., Orth, K. & Salomon, D. (2017) Type VI secretion system MIX-effectors carry both antibacterial and anti-eukaryotic activities. *EMBO Reports*, 18, 1978–1990.

Ruhe, Z.C., Low, D.A. & Hayes, C.S. (2020) Polymorphic toxins and their immunity proteins: diversity, evolution, and mechanisms of delivery. *Annual Review of Microbiology*, 74, 497–520.

Russell, A.B., Hood, R.D., Bui, N.K., LeRoux, M., Vollmer, W. & Mougous, J.D. (2011) Type VI secretion delivers bacteriolytic effectors to target cells. *Nature*, 475, 343–347.

Russell, A.B., Singh, P., Brittnacher, M., Bui, N.K., Hood, R.D., Carl, M.A. et al. (2012) A widespread bacterial type VI secretion effector superfamily identified using a heuristic approach. *Cell Host & Microbe*, 11, 538–549.

Russell, A.B., LeRoux, M., Hathazi, K., Agnello, D.M., Ishikawa, T., Wiggins, P.A. et al. (2013) Diverse type VI secretion phospholipases are functionally plastic antibacterial effectors. *Nature*, 496, 508–512.

Salomon, D., Gonzalez, H., Updegraff, B.L. & Orth, K. (2013) *Vibrio parahaemolyticus* type VI secretion system 1 is activated in marine conditions to target bacteria, and is differentially regulated from system 2. *PLoS One*, 8, e61086.

Salomon, D., Kinch, L.N., Trudgian, D.C., Guo, X., Klimko, J.A., Grishin, N.V. et al. (2014) Marker for type VI secretion system effectors. *Proceedings of the National Academy of Sciences of the United States of America*, 111, 9271–9276.

Schindelin, J., Arganda-Carreras, I., Frise, E., Kaynig, V., Longair, M., Pietzsch, T. et al. (2012) Fiji: an open-source platform for biological-image analysis. *Nature Methods*, 9, 676–682.

Shneider, M.M., Buth, S.A., Ho, B.T., Basler, M., Mekalanos, J.J. & Leiman, P.G. (2013) PAAR-repeat proteins sharpen and diversify the type VI secretion system spike. *Nature*, 500, 350–353.

Shyntum, D.Y., Venter, S.N., Moleleki, L.N., Toth, I. & Coutinho, T.A. (2014) Comparative genomics of type VI secretion systems in strains of *Pantoea ananatis* from different environments. *BMC Genomics*, 15, 163.

Shyntum, D.Y., Theron, J., Venter, S.N., Moleleki, L.N., Toth, I.K. & Coutinho, T.A. (2015) *Pantoea ananatis* utilizes a type VI secretion system for pathogenesis and bacterial competition. *Molecular Plant-Microbe Interactions*, 28, 420–431.

Tang, J.Y., Bullen, N.P., Ahmad, S. & Whitney, J.C. (2018) Diverse NADase effector families mediate interbacterial antagonism via the type VI secretion system. *The Journal of Biological Chemistry*, 293, 1504–1514.

Ting, S.Y., Bosch, D.E., Mangiameli, S.M., Radey, M.C., Huang, S., Park, Y.J. et al. (2018) Bifunctional immunity proteins protect bacteria against FtsZ-targeting ADP-ribosylating toxins. *Cell*, 175, 1380–1392.e14.

Wang, J., Brodmann, M. & Basler, M. (2019) Assembly and subcellular localization of bacterial type VI secretion systems. *Annual Review of Microbiology*, 73, 621–638.

Whitney, J.C., Chou, S., Russell, A.B., Biboy, J., Gardiner, T.E., Ferrin, M.A. et al. (2013) Identification, structure, and function of a novel type VI secretion peptidoglycan glycoside hydrolase effector-immunity pair. *The Journal of Biological Chemistry*, 288, 26616–26624.

Wood, T.E., Howard, S.A., Förster, A., Nolan, L.M., Manoli, E., Bullen, N.P. et al. (2019) The *Pseudomonas aeruginosa* T6SS delivers a periplasmic toxin that disrupts bacterial cell morphology. *Cell Reports*, 29, 187–201.e7.

Wu, C.F., Smith, D.A., Lai, E.M. & Chang, J.H. (2018) The *Agrobacterium* type VI secretion system: a contractile nanomachine for interbacterial competition. *Current Topics in Microbiology and Immunology*, 418, 215–231.

Wu, C.F., Weisberg, A.J., Davis, E.W., 2nd, Chou, L., Khan, S., Lai, E.M. et al. (2021) Diversification of the type VI secretion system in *Agrobacteria*. *mBio*, 12, e0192721.

Zaloba, P., Bailey-Elkin, B.A., Derksen, M. & Mark, B.L. (2016) Structural and biochemical insights into the peptidoglycan hydrolase domain of FlgJ from *Salmonella typhimurium*. *PLoS One*, 11, e0149204.

Zimmermann, L., Stephens, A., Nam, S.-Z., Rau, D., Kübler, J., Lozajic, M. et al. (2018) A completely reimplemented MPI bioinformatics toolkit with a new HHpred server at its core. *Journal of Molecular Biology*, 430, 2237–2243.

SUPPORTING INFORMATION

Additional supporting information can be found online in the Supporting Information section at the end of this article.

How to cite this article: Carobbi, A., Di Nepi, S., Fridman, C.M., Dar, Y., Ben-Yaakov, R., Barash, I. et al. (2022) An antibacterial T6SS in *Pantoea agglomerans* pv. *betae* delivers a lysozyme-like effector to antagonize competitors. *Environmental Microbiology*, 24(10), 4787–4802. Available from: https://doi.org/10.1111/1462-2920.16100